RESEARCH ARTICLE

High Concentrations of Atmospheric Ammonia Induce Alterations in the Hepatic Proteome of Broilers (*Gallus gallus*): An iTRAQ-Based Quantitative Proteomic Analysis

Jize Zhang, Cong Li, Xiangfang Tang, Qingping Lu, Renna Sa, Hongfu Zhang*

State Key Laboratory of Animal Nutrition, Institute of Animal Sciences, Chinese Academy of Agricultural Sciences, Beijing, China

* zhanghf6565@vip.sina.com

Abstract

With the development of the poultry industry, ammonia, as a main contaminant in the air, is causing increasing problems with broiler health. To date, most studies of ammonia toxicity have focused on the nervous system and the gastrointestinal tract in mammals. However, few detailed studies have been conducted on the hepatic response to ammonia toxicity in poultry. The molecular mechanisms that underlie these effects remain unclear. In the present study, our group applied isobaric tags for relative and absolute quantitation (iTRAQ)-based quantitative proteomic analysis to investigate changes in the protein profile change in hepatic tissue of broilers exposed to high concentrations of atmospheric ammonia, with the goal of characterizing the molecular mechanisms of chronic liver injury from exposure to high ambient levels of ammonia. Overall, 30 differentially expressed proteins that are involved in nutrient metabolism (energy, lipid, and amino acid), immune response, transcriptional and translational regulation, stress response, and detoxification were identified. In particular, two of these proteins, beta-1 galactosidase (GLB1) and a kinase (PRKA) anchor protein 8-like (AKAP8 L), were previously suggested to be potential biomarkers of chronic liver injury. In addition to the changes in the protein profile, serum parameters and histochemical analyses of hepatic tissue also showed extensive hepatic damage in ammonia-exposed broilers. Altogether, these findings suggest that longtime exposure to high concentrations of atmospheric ammonia can trigger chronic hepatic injury in broilers via different mechanisms, providing new information that can be used for intervention using nutritional strategies in the future.

Introduction

Ammonia is a colorless, irritant gas generated from the nitrogenous fraction of animal wastes by microbial activity in the broiler house. With the development of the poultry industry,

ammonia as a main contaminant in the air is causing increasing problems with broiler production. The greatest problem caused by ammonia in the air is reduced growth performance, which results in lower body weights and higher feed conversion ratios [1, 2]. Longtime exposure can create severe health issues and interfere with broiler welfare [3, 4].

Ammonia is a toxin in metabolic disorders associated with hyperammonemia, and pro-inflammatory mediators are released into the circulation, modulating the impact of ammonia on the brain tissue [5]. The neurotoxicity of ammonia induces increased expression of tumor necrosis factor α (TNF-α) and interleukin 1 β (IL-1β), which are associated with the production of reactive oxygen species (ROS) and nitric oxide (NO) that are involved with protein kinase A (PKA), the extracellular signal regulated kinase (ERK) pathway and nuclear factor-κB (NF-κB) activation in astrocytes in rats [6]. There is increasing evidence supporting the role of inflammation in exacerbating the neurological manifestations of both acute and chronic liver failure [7].

The liver is a central organ that plays a key role in diverse functions within the body. These functions include regulation of nutrient metabolism (carbohydrate, protein and lipid), immune response, inflammation and removal of xenobiotics [8, 9]. Hepatic function is also strongly influenced by stress and disease [10, 11]. A previous gene array study on broiler chickens demonstrated marked hepatic responses to aqueous ammonia-induced contact dermatitis, including genes associated with energy metabolism, thyroid hormone activity, cellular control and the pro-inflammatory response [3] In rat models of hyperammonemia-induced hepatic injury, microarray results demonstrated that altered expression of hepatic genes was relevant to many vital functions belonging to different signal transduction pathways [12]. To date, most studies of ammonia toxicity have focused on the nervous system and the gastrointestinal tract in mammals. However, few detailed studies have been conducted on the hepatic response to ammonia in poultry.

Numerous studies have demonstrated a lack of correlation between mRNA and protein abundance because of RNA editing and posttranslational modifications [13, 14]. Hence, the elucidation of protein expression is more accurate and imperative [15]. There are numerous enzymes in the liver that are involved in physiological functions related to nutrient metabolism, the immune response, and inflammation, among others [16]. It is almost impossible to detect all of the proteins in hepatic tissue at the same time using traditional methods, such as western blots, immunohistochemical staining or ELISAs. Currently, little is known about the alteration of proteins in the liver of poultry that have been exposed to high levels of atmospheric ammonia.

Based on previous research, we hypothesized that exposure to high concentrations of atmospheric ammonia can confer negative effects on the hepatic tissue of broilers via different mechanisms, which requires further study to elucidate. Therefore, in this study, we utilized a label-based iTRAQ procedure, followed by LC-MS/MS to quantitate altered proteins that are induced differentially in the livers of broilers exposed to high concentrations of atmospheric ammonia.

Materials and Methods

Ethics statement

This study was undertaken in strict accordance with the Regulations for the Administration of Affairs Concerning Experimental Animals of the State Council of the People's Republic of China. The protocol was approved by the Committee on Experimental Animal Management of the Chinese Academy of Agricultural Sciences.

Reagents and chemicals

Protein Assay Kit was purchased from Bio-Rad (Hercules, CA, USA). Reagent for total RNA isolation was from Qiagen (Valencia, CA, USA). Reagents for qPCR were obtained from (Takara, Dalian, China). All iTRAQ reagents and buffers were obtained from Applied Biosystems Inc. (ABI, Foster City, CA). The rest of reagent grade chemicals used in the present study were from Sigma Aldrich (St. Louis, MO, USA) or Fisher Scientific (Pittsburg, PA, USA).

Animals and exposure conditions

Sixty one day old Arbor Acers male broilers were obtained from a commercial hatchery in Beijing (Beijing Arbor Acers Broiler Co., Beijing, China). All birds were housed in individual wire-bottom cages in an environmentally controlled room under standard brooding practices, and given *ad libitum* access to water and a maize-soybean basal diet during the first 21 days. Then, broilers were transferred to environmentally controlled exposure chambers. The diet during the experiment was formulated to achieve the National Research Council (NRC, 1994) recommended requirements for all nutrients containing ME, 12.76 MJ kg^{-1}, and crude protein 19.94% (S1 Table). The concentrated ammonia was delivered in a whole-body animal exposure chamber [4] from days 22 to 42. Each exposure chamber was a 4500 × 3000 × 2500 mm (length × width × height) sealed unit, sectioned for housing 30 birds per chamber. Temperature and airflow were controlled during the exposures to ensure adequate ventilation, minimize buildup of animal-generated contaminants (dander, H_2S, CO_2) and to avoid thermal stress [17].

Broilers in the treatment group were exposed to 75 ± 3 μL/L ammonia during the experimental period. Broilers in the control group were raised in a separate chamber without ammonia for the same period, and the concentration of ambient ammonia was kept at 3 ± 3 μL/L. The concentration of ammonia in both chambers was monitored with a LumaSense Photoacoustic Field Gas-Monitor Innova-1412 (Santa Clara, CA, USA) during the entire experiment. Body weight (BW) and feed consumption were recorded weekly for performance evaluation.

Sample collection

At day 42, all birds were weighed after a 12 h- fasting (12 h food withdrawal) period. Performance parameters (n = 30) including body weight gain, feed intake and feed-conversion ratio were determined. Twelve birds (6 per each group) were randomly selected for blood and hepatic sample collection. The procedure of all sample collections is previously described with slight modifications [12, 18]. Briefly, each blood sample was obtained from a wing vein using a sterilized syringe within 30 s. Blood was incubated in a water bath for 1 h at 37°C then centrifuged at 400 × g for 10 min at 4°C, and the sera obtained were stored at -80°C for further analysis [18]. After blood collection, the chickens were sacrificed by cervical dislocation and then exsanguinated. Then the abdominal and thoracic cavities were opened and hepatic tissues were collected. Small parts of hepatic tissues from both groups were fixed in 10% formaldehyde and used for histochemical analysis. The remaining hepatic samples were then washed with ice-cold sterilized saline, frozen in liquid nitrogen, and stored at -80°C for further proteome and qPCR analyses.

Biochemical and histological analyses

For biochemical analysis, the activities of alanine aminotransferase (ALT), aspartate aminotransferase (AST), creatine kinase (CK) and total superoxide dismutase (T-SOD) in the serum were measured using a corresponding diagnostic kit (Nanjing Jiancheng Bioengineering

Institute, Nanjing, China) according to the instructions of the manufacturer. For histological analysis, the protocol was described previously [18]. Fixed hepatic tissues in 10% phosphate-buffered formalin were processed for paraffin embedding, and 6 μm cross-sections were cut and placed on glass slides. The slides were dewaxed in xylene and rehydrated through gradient ethanol washes and then stained with hematoxylin and eosin (H&E) following standard procedures.

Hepatic sample preparation and protein extraction

Sample pooling is a commonly used strategy to reduce the influence of individual variation on candidate target selection in proteomic studies [19–21]. To avoid erroneous conclusions due to individual variations, the same amount of hepatic tissue sample (weight: weight as 1: 1 ratio) from two chickens in the same group was pooled as a biological replicate, and three biological replicates were acquired for each group.

Hepatic protein extraction was performed as previously described with some modifications [22, 23]. Each pooled hepatic sample (~0.5 g) was ground in a Dounce glass grinder using liquid nitrogen. Ground samples were precipitated with 10% trichloroacetic acid (TCA) (w/v), 90% ice-cold acetone at -20°C for 2 h. The samples were then centrifuged at 20,000 × g for 30 min at 4°C. The supernatants were decanted and the pellets washed with ice-cold acetone. The pellets were lysed in lysis buffer consisting of 8 M urea, 30 mM 4-(2-hydroxyethyl)-1-piperazineethanesulfonic acid (HEPES), 1 mM phenylmethanesulfonyl fluoride (PMSF), 2 mM ethylene diamine tetraacetic acid (EDTA), and 10 mM dithiothreitol (DTT). The undissolved pellets in the crude tissue extracts were removed by centrifugation (20,000 × g, 30 min, 4°C). The tissue lysates were reduced for 1 h at 36°C in a water bath with a final concentration of 10 mM DTT by addition of 1 M DTT and then alkylated for 1 h in the dark with a final concentration of 55 mM by addition of 1 M iodoacetamide (IAM). After reduction and alkylation, 4 volumes of ice-cold acetone was added in the solution in order to precipitate proteins. Then proteins were washed three times with ice-cold pure acetone and resuspended in buffer containing 50% tetraethyl ammonium bromide (TEAB) and 0.1% sodium dodecyl sulfonate (SDS). The undissolved pellets were removed in protein samples by centrifugation (20,000 × g, 30 min, 4°C), and protein quantitation was determined by a Bio-Rad Bradford Protein Assay Kit (Hercules, CA, USA).

Trypsin digestion

Each sample was digested overnight at 37°C adding sequencing grade trypsin (Promega Corporation, Madison, WI) at a 1: 30 ratio (3.3 μg trypsin: 100 μg target) [22].

iTRAQ labeling

iTRAQ labeling procedure was described in previous report [22]. Protein samples in the control group were labeled with iTRAQ tags (solubilized in 70 μL isopropanol prior to use) 113, 114 and 115 while treatment samples received iTRAQ tags 116, 117, and 121. All labeled samples (organic composition > 60% by adding isopropanol) were incubated at room temperature for 2 h.

Strong cation exchange chromatography

The strong cation exchange fractionation protocol followed previous reports [20, 23, 24] with slight modifications. Briefly, total amount of 600 μg sample was loaded onto a strong cation exchange column (Phenomenex Luna SCX 100A) equilibrated with buffer A (10 mM KH_2PO_4 in

25% acetonitrile, pH 3.0) using an Agilent 1100 (Santa Clara, CA) system. The peptides were separated using a linear gradient of buffer B (10 mM KH_2PO_4 and 2 M KCl in 25% acetonitrile, pH 3.0) increasing to 5% after 41 min, 50% after 66 min and 100% after 71 min, at a flow rate of 1 ml/min. Elution was monitored by measuring the absorbance at 214 nm. Total of 16 fractions were collected from the eluted peptides, and each fraction was desalted with a Strata X C18 column (Phenomenex) and vacuum-dried.

Mass spectrometry

The protocol of MS analysis was described previously with slight modifications [20]. Each fraction was redissloved in buffer A (2% acetonitrile, 0.1% formic acid) and centrifuged at $20,000 \times g$ for 10 min. The final concentration of peptides in each fraction was approximately 0.25 µg/µl on average. Twenty microliter of supernatant was loaded onto an UltiMate 3000 Nano LC system (Bannockburn, IL) by the auto sampler onto a C18 trap column (length 2 cm, inner diameter 200 µm). Peptides were eluted onto a resolving analytical C18 column (length 10 cm, inner diameter 75 µM, 5-µm particles, 300 Å) packed in-house. Samples were loaded at 15 µl/min for 4 min and eluted with a 45-min gradient at 400 nl/min from 5 to 60% buffer B (98% acetonitrile, 0.1% formic acid), separated with a 3- min linear gradient to 80% B, maintained at 80% B for 7 min, and finally returned to 5% B over 3 min. The peptides were subjected to nanoelectrospray ionization followed by tandem mass spectrometry (Q-Exactive, Thermo) coupled online to the nanoLC. Intact peptides were detected in the Orbitrap at a resolution of 70,000 full with width at half maximum (FWHM). Peptides were selected for MS/MS using high-energy collision dissociation (HCD) operating mode with a normalized collision energy setting of 28%; ion fragments were detected in the Orbitrap at 17,500 FWHM resolution. A data-dependent acquisition mode that alternated between a MS scan followed by MS/MS scans was applied for the 10 most abundant precursor ions (2^+ to 4^+) above a threshold ion count of 20,000 in the MS survey scan with a following Dynamic Exclusion duration of 15 s (isolation window of m/z 2.0 and a maximum ion injection time of 100 ms). The electrospray voltage applied was 1.8 kV. Automatic gain control (AGC) was used to optimize the spectra generated by the Orbitrap. The AGC target for full MS was 3E6 and 1E5 for MS2. For MS scans, the m/z scan range was 350 to 2000. For MS2 scans, the m/z scan range was 100–1800.

Data processing and analyses

MS/MS data for iTRAQ protein identification and quantitation were analyzed using Proteome Discover 1.3 (Thermo Fisher Scientific) and searched with in-house MASCOT software (Matrix Science, London, U.K.; version 2.3.0) against the database Uniprot_Gallus gallus_9031 (Apr 11th, 2014 with 29,020 protein sequences) with the following parameters: enzyme: trypsin; fixed modification: carbamidomethyl (C); variable modifications: oxidation (M), gln-pyro-glu (N-term Q), iTRAQ 8-plex (N-term, K, Y); peptide mass tolerance:15 ppm; MS/MS tolerance: 20 mmu; maximum missed cleavages: 1. Identified peptides had an ion score above the threshold of peptide identity established by Mascot, and protein identifications were accepted within the false discovery rate (FDR) of 1% in which at least one such unique peptide match was specific for the protein. Median ratio normalization was performed in intra-sample channels in order to normalize each channel across all proteins. Protein quantitative ratios for each iTRAQ labeled sample were obtained, using a pooled sample in the control group (sample tagged with 113) as the denominator. Quantitative ratios were then log transformed to base 2 and presented as fold change relative to the denominator in the control group for final quantitative testing. Differentially expressed proteins were determined using Student's t-test corrected for multiple testing performing the Benjamini and Hochberg correction [25]. Proteins with a

1.2-fold change or greater were considered to be differentially expressed. The mass spectrometry proteomics data have been deposited to the ProteomeXchange Consortium (http://proteomecentral.proteomexchange.org) via the PRIDE partner repository with the dataset identifier PXD001670.

Bioinformatics analysis of proteins differential abundance

Gene Ontology (GO) distribution for all of the proteins that were significantly altered in hepatic samples of ammonia-exposed chickens were classified using Blast2GO software (http://www.blast2go.com/) and WEGO (http://wego.genomics.org.cn) that were provided by the Institute for Genomic Research [26, 27]. Database for Annotation, Visualization and Integrated Discovery (DAVID) 6.7 (http://david.abcc.ncifcrf.gov/) and the Kyoto encyclopedia of genes and genomes (KEGG) data base (released December 2014), were used to classify differentially expressed proteins in significantly overrepresented pathways and GO terms.

Validation of proteins of differential abundance

Real-time quantitative PCR (qPCR) was used to verify eight hepatic tissue proteins of differential abundance at the mRNA level by the method previously described [18] with slight modifications. Total RNA from hepatic tissue samples was isolated using Qiagen RNeasy Plus Mini Kit (Valencia, CA). Agarose gel electrophoresis was used to test the RNA quality. And the RNA quantity was verified with a spectrophotometer (Nanodrop 2000, Thermo Scientific, Waltham, MA). Then total RNA was reverse transcribed using the Reverse Transcriptase, D2680A (Takara, Dalian, China). All mRNA expression levels were analyzed by RT-qPCR using the RT reagent Kit, RR037A (SYBR Green) (Takara, Dalian, China) and an Applied Biosystems 7500 Fast Real-Time PCR System (Foster City, CA). RT-qPCRs are performed as the following conditions: 95°C for 30 s, 40 cycles of 95°C for 10 s and 60°C for 30 s. Fluorescence data were detected at the last step of each cycle to monitor the amount of PCR product. The Primer sequences are shown in S2 Table. The relative fold-change was calculated by the $2^{-\Delta\Delta CT}$ method [18].

Statistical analysis

Data on growth performance, serum parameters and gene expressions were analyzed by one-way ANOVA (SAS Version 9.2, SAS institute Inc., Cary, NC). A group difference was assumed to be statistically significant when $P < 0.05$. All results were expressed as means ± S.D.

Results

Effect of high concentrations of atmospheric ammonia on the growth performance of broilers

In this study, treatment for all birds (control and treatment group) began on day 22. During the entire experimental period (20 days), birds exposed to ammonia had 15.4% less ($P < 0.05$) average daily gain (ADG) and 9.6% less ($P < 0.05$) average daily feed intake (ADFI). On the contrary, the feed conversion ratio (FCR) for the treatment group was greatly increased ($P < 0.05$) compared with the control group (Table 1).

Table 1. Effect of atmospheric ammonia on the growth performance of broilers.

	Groups	
	Control	**Treatment**
ADG (g/d)	91.08 ± 3.58[a]	77.03 ± 2.51[b]
ADFI (g/d)	149.45 ± 1.87[a]	135.14 ± 2.79[b]
FCR (g feed/g weight gain)	1.64 ± 0.09[b]	1.75 ± 0.05[a]

ADG, average daily gain; ADFI, average daily feed intake; FCR, feed conversion ratio. Values within a row not sharing a common superscript letter indicate significant difference at $P < 0.05$. Numbers are mean ± S.D. (n = 30).

doi:10.1371/journal.pone.0123596.t001

Effect of high concentration of atmospheric ammonia on the serum parameters and histochemistry of hepatic sample

In the treatment group, activities of serum ALT, AST and CK were significantly elevated ($P < 0.05$) compared with the control group indicating extensive hepatic injury (Table 2). Anti-oxidase T-SOD and the serum level of ALB were decreased significantly compared with the control group ($P < 0.05$), illustrating lower oxidation resistance and synthetic capability (Table 2). For histological analysis, no obvious histological abnormalities were noted in the control group (Fig 1A). Compared with control broilers, the hepatocytes of ammonia-exposed broilers (Fig 1B) exhibited widespread vacuole degeneration.

Identification and comparison of proteins of differential abundance

Using iTRAQ analysis, a total of 79,527 peptide spectral matches were found, and 2452 proteins were identified within the FDR of 1% (S3 Table). Following statistical analysis, 34 proteins were found to be differentially expressed in hepatic tissue between the control and treatment groups, with 21 being up-regulated and 13 down-regulated (S4 Table).

A total of 30 proteins of differential abundance were grouped into eight classes based on putative functions: stress response and detoxification (23.3%), transcriptional and translational regulation (20.0%), immune response and inflammation (13.3%), miscellaneous (16.7%), energy metabolism (6.7%), lipid metabolism (6.7%), amino acid metabolism (6.7%) and markers of hepatic injury (6.7%) (Fig 2). Those related to stress response and detoxification, transcriptional and translational regulation, and immune response and inflammation were predominant and accounted for over 50% of the differentially- expressed proteins. A comparison of proteins

Table 2. Effect of atmospheric ammonia on the serum biochemical parameters of broilers.

	Groups	
	Control	**Treatment**
ALT (IU/L)	19.33 ± 1.14[b]	24.87 ± 1.25[a]
AST (IU/L)	239 ± 5.18[b]	291 ± 5.65[a]
ALB (g/L)	14.75 ± 0.77[a]	11.45 ± 0.52[b]
CK (U/L)	6224.50 ± 172.26[b]	7173.63 ± 309.05[a]
T-SOD (U/mL)	77.81 ± 6.55[a]	61.12 ± 2.11[b]

ALT, activity of alanine aminotransferase; AST, activity of aspartate aminotransferase; ALB, albumin; CK, creatine kinase; T-SOD, total superoxide dismutase. Values within a column not sharing a common superscript letter indicate significant difference at $P < 0.05$. Numbers are mean ± S.D. (n = 6).

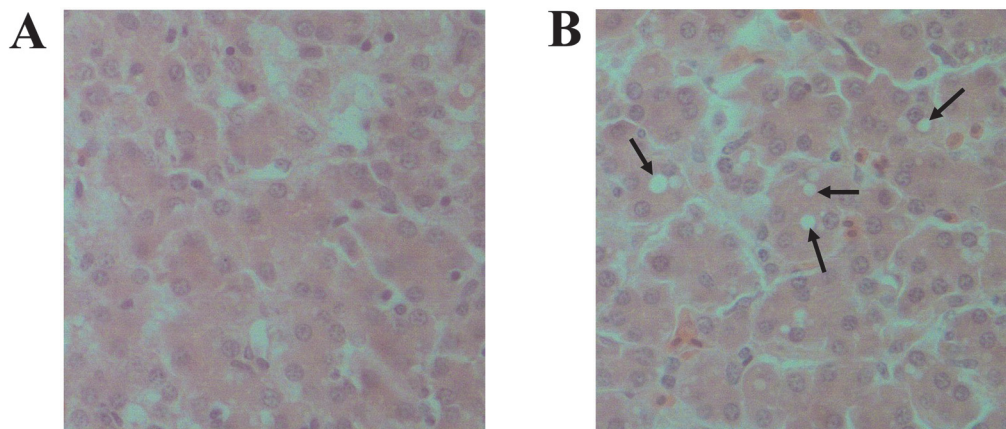doi:10.1371/journal.pone.0123596.t002

Fig 1. Histochemical examination of hepatic samples from broilers. Livers were fixed overnight in 10% phosphate-buffered formalin, and the tissue sections were prepared for hematoxylin and eosin staining. Representative images were captured by a microscope (Olympus BX51, Japan) at 400×; (A) CTRL, control group (3 ± 3 µL/L ammonia), (B) TRET, treatment group (75 ± 3 µL/L ammonia). In the TRET group, hepatocytes exhibited vacuole degeneration (arrow).
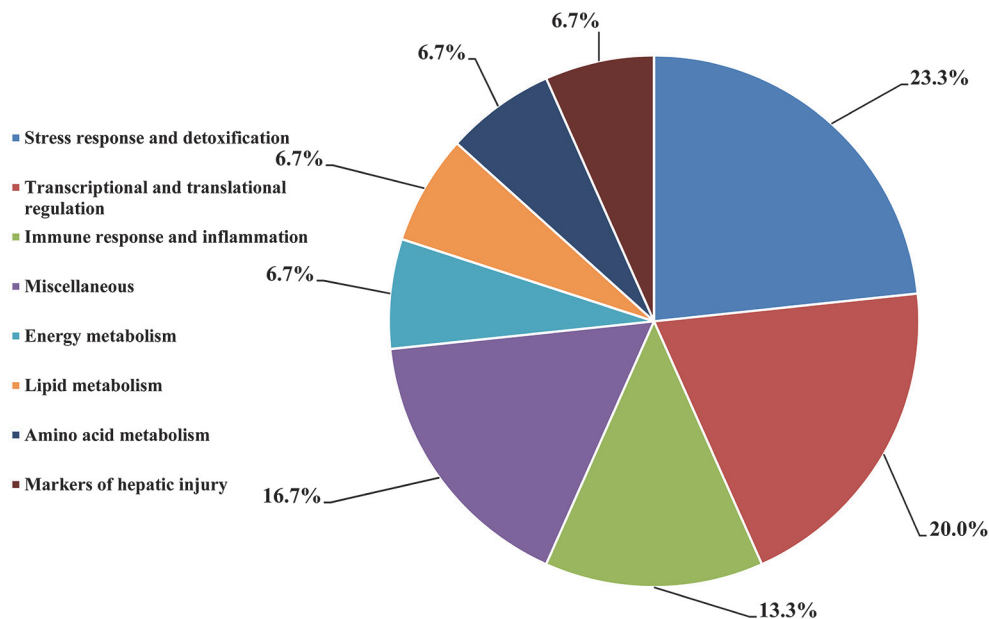
Fig 2. Functional classification of the proteins of differential abundance identified from the hepatic tissues of 42-day-old broilers.

of differential abundance with functional grouping between the two groups indicated that more protein species were up- regulated in ammonia-exposed chickens (18 versus 12, respectively) (Table 3). These 18 up-regulated protein species were distributed in six categories: five in stress response and detoxification, three in transcriptional and translational regulation, three in miscellaneous, two in lipid metabolism, two in amino acid metabolism and two in markers of hepatic injury (Table 3). The 12 down-regulated protein species were distributed in five categories: three in transcriptional and translational regulation, three in immune response and inflammation, two in stress response and detoxification, two in energy metabolism and two in miscellaneous. Most importantly, two protein species, beta-1 galactosidase (GLB1) and a kinase (PRKA) anchor protein 8-like (AKAP8 L), previously identified as potential biomarkers of hepatic injury, were found to be up-regulated in ammonia-exposed broilers in the present study.

GO annotations and pathway analysis

In the cellular component group, the differentially expressed proteins are concentrated in intracellular organelles and the cytoplasm (Fig 3). In the molecular functional group, the differentially expressed proteins that are metabolic enzymes (oxidoreductase activity and hydrolase activity), binding proteins (protein binding and ion binding) and transporter (transmembrane), were ranked at the top of the category occupancy, suggesting that the relevant functions were important in the livers of broilers (Fig 3). In the biological process category, the proteins that participate in cellular processes (protein metabolic process), metabolism (protein and energy metabolism) and biological regulation (regulation of immune process), were at the top ratio in the differentially expressed proteins (Fig 3), suggesting that exposure to ammonia results mainly in changes in protein, energy metabolism and immune function.

In addition, GO annotation and KEGG pathway enrichment analysis were used to determine the overrepresented biological events and to provide a primary overview of the hepatic proteome influenced by exposure to ammonia. The DAVID 6.7 software identified that oxidation reduction in the biological process category is highly overrepresented (Table 4). The following proteins involved in this GO term were found to be enriched: TBXAS1, UQCRH, FADS1, ACAD9 and FTH1. These proteins might participate in the oxidation related metabolism. This functional enrichment analysis result indicated that exposure of ammonia had effect on oxidation system of chicken liver. KEGG pathway enrichment analysis of the differential proteins revealed information about protein functions in the metabolism pathway [21]. KEGG analysis showed that four differentially expressed proteins including MAN2B2, GLB1, TPP1 and M6PR, were significantly enriched in the two identified pathways. These proteins were involved in glycan degradation and lysosome (Table 4).

Validation of proteins of differential abundance

Eight differentially expressed proteins (AKAP8 L and GLB1 as potential biomarkers of hepatic injury, C6 and IGJ involved in immune response, FADS1 involved in lipid metabolism, MCMBP involved in transcriptional and translational regulation, MAP2K6 involved in receptor signaling, and FTH1 involved in stress response) were selected for validation of proteomic data at the mRNA level using qPCR (Fig 4). The protein levels of AKAP8 L, GLB1, C6, FADS1, MCMBP and MAP2K6 were consistent with their mRNA expression levels. The results for the remaining two proteins were inconsistent between the mRNA levels and the protein levels. Possible reasons for these inconsistent results include the following: 1) the relationships between the mRNA levels and the protein levels were indirect that some proteins were encoded by more than one gene, 2) there were some post-translational effects and/or the function of

Table 3. List of differentially expressed nutrients metabolic proteins in hepatic samples from treatment group and control group.

Accession	Description	Gene name	Log₂ fold change	P-value	Biological process GO term
Energy metabolism					
Q5ZJ68	Uncharacterized protein OS = Gallus gallus GN = RCJMB04_20f2 PE = 2 SV = 1 - [Q5ZJ68_CHICK]	ACAD9	-0.29	0.0189	Acyl-CoA dehydrogenase activity
F1NSI8	Uncharacterized protein OS = Gallus gallus PE = 4 SV = 2 - [F1NSI8_CHICK]	None	-0.28	0.0420	GTP binding
Lipid metabolism					
E7EDS8	Fatty acid desaturase 1 OS = Gallus gallus GN = FADS1 PE = 2 SV = 1 - [E7EDS8_CHICK]	FADS1	0.31	0.0050	Fatty acid biosynthetic process
E1BYN1	Uncharacterized protein OS = Gallus gallus GN = LOC100858955 PE = 4 SV = 2 - [E1BYN1_CHICK]	LOC769339	0.42	0.0001	Fatty acid biosynthesis
Amino acid metabolism					
E1BZY3	Uncharacterized protein (Fragment) OS = Gallus gallus GN = A2LD1 PE = 4 SV = 2 - [E1BZY3_CHICK]	A2 LD1	0.35	0.0149	Cellular modified amino acid catabolic process
E1C9D0	Uncharacterized protein OS = Gallus gallus GN = DDO PE = 4 SV = 1 - [E1C9D0_CHICK]	DDO	0.39	0.0315	D-amino acid catabolic process
Transcriptional and translational regulation					
H9KZJ3	Uncharacterized protein OS = Gallus gallus PE = 4 SV = 2 - [H9KZJ3_CHICK]	None	-0.46	0.0242	Histone deacetylase activity
P09987	Histone H1 OS = Gallus gallus PE = 1 SV = 2 - [H1_CHICK]	None	-0.35	0.0284	DNA binding
F1NXK0	Mini-chromosome maintenance complex-binding protein OS = Gallus gallus GN = MCMBP PE = 4 SV = 2 - [F1NXK0_CHICK]	MCMBP	-0.32	0.0439	Chromatin binding
F1P4I9	Proteasomal ubiquitin receptor ADRM1 OS = Gallus gallus GN = ADRM1 PE = 2 SV = 1 - [F1P4I9_CHICK]	ADRM1	0.29	0.0299	Proteasome assembly
E1BUS2	Uncharacterized protein OS = Gallus gallus GN = NOP58 PE = 4 SV = 2 - [E1BUS2_CHICK]	NOP58	0.32	0.0425	snoRNA binding
F1N8A7	Uncharacterized protein OS = Gallus gallus GN = RBKS PE = 4 SV = 2 - [F1N8A7_CHICK]	RBKS	0.34	0.0182	Ribokinase activity
Immune response and inflammation					
E1BY93	Uncharacterized protein OS = Gallus gallus GN = IGJ PE = 4 SV = 1 - [E1BY93_CHICK]	IGJ	-0.38	0.0126	IgA binding
F1NIU6	Uncharacterized protein OS = Gallus gallus GN = M6PR PE = 2 SV = 2 - [F1NIU6_CHICK]	M6PR	-0.33	0.0362	Mannose transmembrane transporter activity
B8ZX71	Sixth complement component OS = Gallus gallus GN = C6 PE = 2 SV = 1 - [B8ZX71_CHICK]	C6	-0.28	0.0120	Innate immune response
F1NE09	Uncharacterized protein OS = Gallus gallus GN = CYFIP2 PE = 4 SV = 2 - [F1NE09_CHICK]	CYFIP2	0.29	0.0288	Protein binding
Stress response and detoxification					
H9KZK9	Uncharacterized protein OS = Gallus gallus PE = 4 SV = 2 - [H9KZK9_CHICK]	None	-0.50	0.0006	Scavenger receptor activity
F1P4G4	Uncharacterized protein OS = Gallus gallus GN = TBXAS1 PE = 3 SV = 2 - [F1P4G4_CHICK]	TBXAS1	-0.35	0.0101	Oxidoreductase activity
D0VX28	Cytochrome b-c1 complex subunit 6 OS = Gallus gallus PE = 1 SV = 1 - [D0VX28_CHICK]	UQCRH	0.31	0.0290	Mitochondrial electron transport
E1BUZ3	Uncharacterized protein OS = Gallus gallus GN = DHRS12 PE = 4 SV = 2 - [E1BUZ3_CHICK]	DHRS12	0.32	0.0079	Short-chain dehydrogenases activity
F1NMA3	Sulfotransferase family cytosolic 1B member 1 OS = Gallus gallus GN = SULT1B1 PE = 4 SV = 2 - [F1NMA3_CHICK]	SULT1B1	0.33	0.0336	Sulfotransferase activity

(Continued)

Table 3. (*Continued*)

Accession	Description	Gene name	Log$_2$ fold change	*P*-value	Biological process GO term
P08267	Ferritin heavy chain OS = Gallus gallus GN = FTH PE = 2 SV = 2 - [FRIH_CHICK]	FTH1	0.52	0.0068	Ferroxidase activity
E1C004	Uncharacterized protein (Fragment) OS = Gallus gallus GN = CA4 PE = 4 SV = 2 - [E1C004_CHICK]	CA4	0.64	0.0245	Carbonate dehydratase activity
Marker of hepatic injury					
Q5ZLM4	Uncharacterized protein OS = Gallus gallus GN = GLB1 PE = 2 SV = 1 - [Q5ZLM4_CHICK]	GLB1	0.26	0.0163	Beta-galactosidase activity
H9L081	Uncharacterized protein OS = Gallus gallus GN = AKAP8L PE = 4 SV = 2 - [H9L081_CHICK]	AKAP8 L	0.30	0.0444	DNA binding
Miscellaneous					
F1NDH2	Angiotensinogen OS = Gallus gallus GN = AGT PE = 3 SV = 2 - [F1NDH2_CHICK]	AGT	-0.37	0.0189	Acetyltransferase activator activity
F1NDD1	Uncharacterized protein (Fragment) OS = Gallus gallus GN = SFXN2 PE = 4 SV = 2 - [F1NDD1_CHICK]	SFXN2	-0.35	0.0102	Aation transmembrane transporter activity
F1NB83	Uncharacterized protein (Fragment) OS = Gallus gallus GN = TPP1 PE = 4 SV = 2 - [F1NB83_CHICK]	TPP1	0.32	0.0153	Serine-type endopeptidase activity
F1NQF6	Uncharacterized protein OS = Gallus gallus GN = MAN2B2 PE = 4 SV = 2 - [F1NQF6_CHICK]	MAN2B2	0.36	0.0212	Mannosidase activity
F1NVF2	Uncharacterized protein OS = Gallus gallus GN = MAP2K6 PE = 4 SV = 2 - [F1NVF2_CHICK]	MAP2K6	0.32	0.0105	MAP kinase kinase activity

A total of 30 proteins of differential abundance were grouped into eight classes based on putative functions. Protein expressions are represented as log$_2$ fold change relative to the control

doi:10.1371/journal.pone.0123596.t003

other regulatory mechanisms such as ubiquitin, proteolysis, regulation of microRNA and so on [13, 14], and 3) there was a time delay between responses on the mRNA and protein levels [21].

Discussion

The liver is an important organ for nutrient metabolism and detoxification. Any damage to hepatocytes can trigger severe healthy issues in the body. Whether an exposure to high concentrations of ammonia has a direct effect on the functional hepatocytes, thereby causing synthetic and metabolic disorder of broiler's liver, remains unknown. Much less is understood regarding the molecular mechanism of hepatic injury in poultry induced by exposure to atmospheric ammonia. In the present study, iTRAQ-based quantitative proteomic analysis integrated with biochemical detections was performed to investigate the hepatic response in ammonia-exposed broilers.

Serum levels of ALT, AST and CK serve as important indicators of hepatic function and were found to be significantly higher in ammonia-exposed broilers, indicating that ammonia exposure severely impaired hepatic function. In addition, lower levels of T-SOD and ALB in the serum of the treatment group suggested that the hepatic injury was associated with oxidative stress and disorders of synthetic functions. The result of histochemical analysis was consistent with changes of serum parameters and showed that a proportion of hepatocytes began to display widespread vacuole degeneration in ammonia-exposed broilers.

As an essential metabolic organ, the liver plays a vital rule in the production of ATP, which is involved in a number of physiological processes. However, ATP production is usually found to be impaired in animal models of hepatic injury. In hepatic cirrhosis patients, although
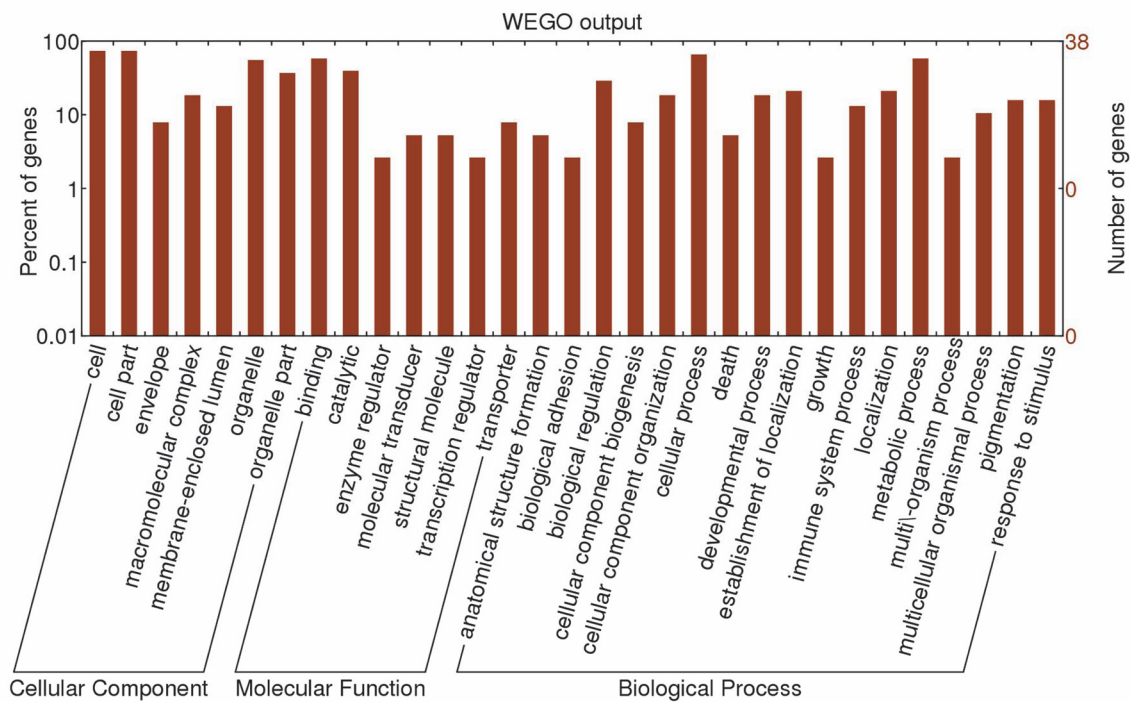
Fig 3. GO distribution analysis of differentially expressed proteins in hepatic tissues from treatment group and control group. The number of proteins for each GO annotation is shown in right axis, and the proportion of proteins for each GO annotation is exhibited in left axis.

mitochondrial function and ATP generation were maintained by increasing energy production from glycolytic flux at an early phase, mitochondria respiration and ATP production were significantly compromised at the terminal stage of hepatic injury [28]. Chronic administration of toxins that induce hepatic damage in a mouse model demonstrated that liver ATP-content was reduced to 58% of controls after 2 weeks of intoxication [29]. Both decreased glycolytic and mitochondrial ATP production were also demonstrated in a chronic alcoholic liver injury model [30]. These results are consistent with our discovery that abundances of the proteins encoded by acyl-CoA dehydrogenase gene (ACAD9) and a GTP binding protein (Uniport database accession F1NSI8) related to energy production [31] were down-regulated in hepatic samples of ammonia- exposed broilers. GO annotation enrichment analysis of the present study also

Table 4. Enriched KEGG pathway-based sets and GO terms of proteins of differential abundance in the hepatic tissue of broilers.

Category	Term	Count	Genes	P value
GO term	Oxidation reduction	5	TBXAS1, UQCRH, FADS1, ACAD9, FTH1	0.0042
KEGG pathway	Other glycan degradation	2	MAN2B2, GLB1	0.0489
KEGG pathway	Lysosome	3	TPP1, M6PR, GLB1	0.0499

ACAD9, acyl-CoA dehydrogenase family, member 9; FADS1, fatty acid desaturase 1; FTH1, ferritin heavy chain; GLB1, galactosidase, beta 1; MAN2B2, mannosidase, alpha, class 2B, member 2; M6PR, mannose-6-phosphate receptor; TBXAS1, thromboxane A synthase 1; TPP1, tripeptidyl peptidase I; UQCRH, ubiquinol-cytochrome C reductase hinge protein; The number of count refers to the amount of proteins involved in the extended KEGG network and pathway. P values are calculated according to a modified Fisher's exact test and corrected for multiple testing using the Bonferroni correction provided by DAVID.
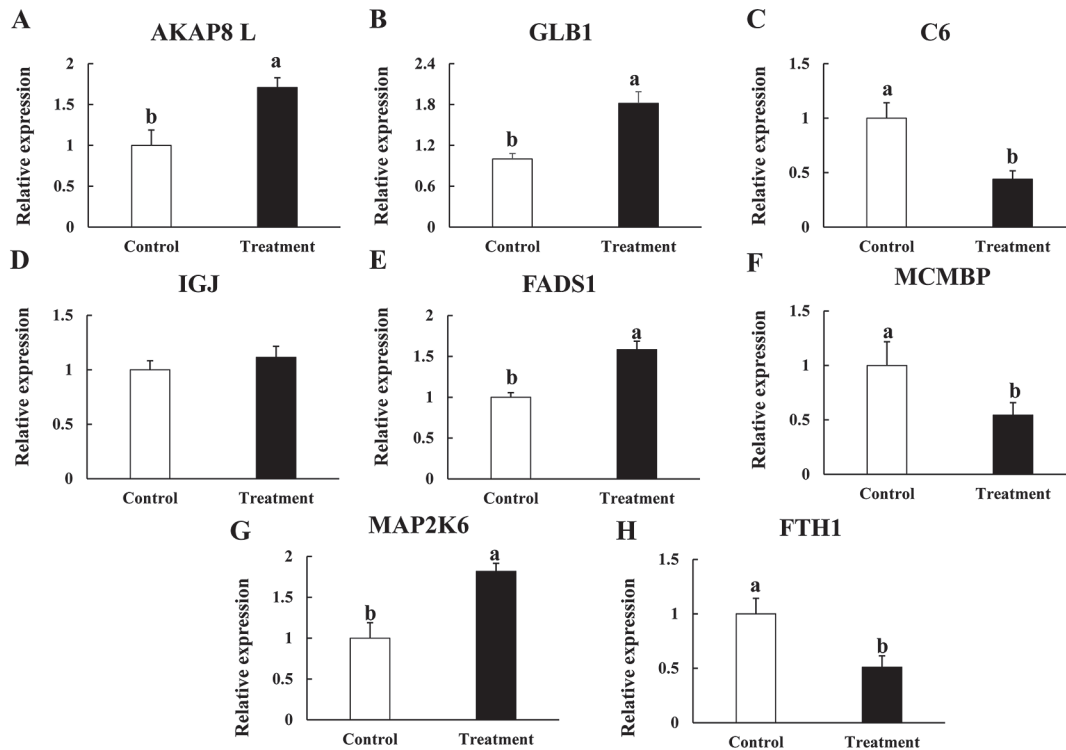
Fig 4. qPCR validation of eight proteins of differential abundance from the hepatic tissues of 42-day-old AA broilers at the mRNA level (A, B, C, D, E, F, G and H). Samples were normalized with the reference gene β-actin. Data are presented as means ± S.D (n = 6 per group). Mean values with different superscript letters ([a, b]) are significantly different ($P < 0.05$).

showed that oxidation reduction term is overrepresented in hepatic proteome of ammonia- exposed broilers. Additional determinations are still required on physiological parameters such as ATP content, oxidative phosphorylation and so on in the future.

FADS1 participates in hepatic lipogenesis and catalyzes the conversion of long chain saturated fatty acids to monounsaturated fatty acids [32, 33]. The protein encoded by the fatty acyl-CoA hydrolase precursor gene (LOC769339) has been investigated previously, and its induction represents an adaptive response to fatty acid overload in the liver of animals fed a high-fat diet [34]. A previous study demonstrated that accumulation of fat in hepatocytes was shown in broilers raised under higher concentration of ammonia [35]. Up-regulation of these two proteins was observed in livers of ammonia- exposed birds and is consistent with the previous research. However, direct evidence is still required, such as fat content and profile of fatty acids, which will be involved in the additional study in the future.

Amino acid metabolism is one of the key functions in the liver and is an important indicator of the health status of hepatocytes. A2 LD1 (AIG2-like domain 1) is involved in proteolytic degradation, which is considered to be a biomarker in amniotic fluid during gestosis [36]. DDO (D-aspartate oxidase) acts as a detoxifying agent to metabolize D-amino acids [37]. Up-regulation of these two proteins indicates that exposure to ammonia may trigger perturbations in amino acid metabolism in hepatocytes. The determination of hepatic profile of amino acids will be considered in further study.

Transcriptional and translational regulatory proteins have crucial roles in the growth, proliferation and differentiation of hepatocytes. In this study, six differentially expressed protein

species related to transcriptional and translational regulation were up- and down-regulated in the treatment group, respectively. Histone H1 and a histone deacetylase protein (Uniport database accession H9KZJ3) are involved in the regulation of gene expression, and down-regulation of both proteins was reported to be associated with impairment of liver regeneration [38]. MCMBP is known to be crucial for DNA replication, regulating initiation and elongation of DNA and providing DNA helicase activity [39]. ADRM1 is an integral plasma membrane protein that promotes cell adhesion, which has been shown to be induced in hepatocellular carcinoma (HCC) [40]. NOP58 (NOP58 ribonucleoprotein) is essential for ribosomal biogenesis, whereas an increased expression of this protein was observed in hyperglycemia-induced vascular injury [41, 42]. RBSK (ribokinase) is an important component of the first step of ribose metabolism; however, its elevated expression was demonstrated in livers of patients having pancreatic cancer metastasis [43]. Down-regulation of histones and MCMBP, together with up-regulation of ADRM1, NOP58 and RBSK observed in the present study, indicates that proliferation of normal hepatocytes was restrained, whereas the number of aberrant hepatocytes was increased.

In addition to having roles in nutrient metabolism, the liver is also an important organ for immunity and detoxification *in vivo*. In this study, 11 differentially-expressed proteins were identified in the categories of immune response, stress response and detoxification. Of these proteins, IGJ is active during the early stages of both B and T cell differentiation [44]; M6PR (mannose-6-phosphate receptor) plays a critical role in lysosome function through the specific transport of mannose-6-phosphate-containing acid hydrolases from the Golgi complex to lysosomes [45]; C6 reduces risks for disseminated Neisserial infections [46]. Down-regulation of immune and anti-inflammatory response-related proteins in this study indicates that the immunity of ammonia-exposed broilers was diminished, which renders broilers susceptible to bacterial or viral infections. However, up-regulation of apoptosis related CYFIP2 (cytoplasmic FMR1-interacting protein 2) may trigger the death of hepatocytes in the treatment group [47]. Furthermore, protein species related to oxidative stress and detoxification were up- and down-regulated in ammonia-exposed broilers, respectively. Elevated abundances of protein related to oxidative stress, including UQCRH, SULT1B1, CA4 (carbonic anhydrase 4), DHRS12 (dehydrogenase/reductase (SDR family) member 12) and FTH1 were observed in the present study. Up-regulation of these proteins is closely related to the formation of reactive oxygen species [48–51]. Together with the result of decreased serum level of T-SOD in the treatment group, we conclude that the exposure to ammonia induces oxidative stress in hepatocytes. This behavior is consistent with the increased oxidative stress in astrocytes induced by the neurotoxicity of ammonia [6]. In contrast, down-regulation of a scavenger receptor protein (Uniport database accession H9KZK9) involved in detoxification was demonstrated in the treatment group [52]. We speculate that the ability to remove xenobiotics may be impaired in hepatocytes of ammonia-exposed broilers.

Notably, two proteins previously identified as potential biomarkers of hepatic injury were found to be differentially expressed in the present study. GLB1 is a member of a group of enzymes that are contained predominantly within lysosomes and are released during Kupffer cell activation or death. It has been proposed as a marker of liver injury induced by radiation [53]. A rapid elevation of GLB levels corresponded well with impaired liver function and extensive hepatic injury [54]. AKAP8 L is involved in nuclear envelope breakdown and chromatin condensation. In high glucose induced diabetic liver disease, AKAP8 L was regarded as a potential marker of diabetic liver diseases [55]. Both proteins were greatly up-regulated in livers of ammonia-exposed broilers. Thus, we suggest that GLB1 and AKAP8 L are potential biomarkers of ammonia induced chronic hepatic injury in broilers.

In addition to the aforementioned protein clusters, differential abundances of several proteins involved in a broad array of functions were observed in this study. Of these proteins, MAP2K6 (mitogen-activated protein kinase kinase 6) plays a crucial role in the p38 MAP kinase signal cascade that regulates various stress-induced responses under pathological conditions [17, 56]. Previous research has demonstrated that the stress-activated MAPK cascade and p38 were main factors in chronic liver injury in hepatocarcinogenesis [57, 58]. An increased abundance of MAP2K6 was observed in our study, which indicates that the mechanism of ammonia-related liver injury may be related to the MAP kinase (MAPK) signaling pathway. However, this speculation is only derived from the present study and requires a huge effort to prove in further research. As similar as GLB1, TPP1 (tripeptidyl peptidase I) is also an important lysosomal protease [59]. KEGG pathway analysis in the present study showed that both proteins are involved in lysosome. This observation indicates that lysosome may play a vital role in hepatocytes of ammonia-exposed broilers.

In summary, the present proteomic analysis has demonstrated that exposure to high concentrations of atmospheric ammonia leads to differential abundances of a number of hepatic proteins in broilers. The functional groupings of those altered proteins are mainly related to stress response, immunity, and transcriptional and translational regulation. Some other proteins involved in nutrient metabolism (energy, lipid and amino acid), and receptor signaling were also differentially expressed. Most importantly, two proteins (GLB1 and AKAP8 L) previously identified as potential biomarkers of hepatic injury, were found in ammonia-exposed broilers. Altogether, the results of proteomic, biochemical and histological analyses, suggest that exposure to high concentrations of atmospheric ammonia triggers severe chronic hepatic injury through oxidative stress and some other ways in broilers. Future studies will investigate the regulatory mechanisms responsible for attenuating damages induced by atmospheric ammonia.

Supporting Information

S1 Table. Composition of the experimental diet and calculated proximate composition of the diet.
(DOC)

S2 Table. The qPCR primers used for verification of the differentially expressed genes of the AA broiler hepatic tissues.
(DOC)

S3 Table. List of all proteins (n = 2452) identified in the study.
(XLS)

S4 Table. List of all differentially expressed proteins (n = 34) identified in the study.
(XLS)

Acknowledgments

Author Contributions

Conceived and designed the experiments: JZZ CL HFZ. Performed the experiments: JZZ CL. Analyzed the data: JZZ CL QPL RNS. Contributed reagents/materials/analysis tools: JZZ XFT QPL RNS. Wrote the paper: JZZ HFZ.

References

1. Miles DM, Branton SL, Lott BD. Atmospheric ammonia is detrimental to the performance of modern commercial broilers. Poult Sci. 2004; 83: 1650–1654. PMID: 15510548

2. Shlomo Y. Ammonia affects performance and thermoregulation of male broiler chickens. Anim Res. 2004; 53: 289–293.

3. Sherlock L, McKeegan DE, Cheng Z, Wathes CM, Wathes DC. Effects of contact dermatitis on hepatic gene expression in broilers. Br Poult Sci. 2012; 53: 439–452. doi: 10.1080/00071668.2012.707310 PMID: 23130578

4. Wei FX, Xu B, Hu XF, Li SY, Liu FZ, Sun QY, et al. The effect of ammonia and humidity in poultry houses on intestinal morphology and function of broilers. J Anim Vet Adv. 2012; 11: 3641–3646.

5. Skowrońska M, Albrecht J. Oxidative and nitrosative stress in ammonia neurotoxicity. Neurochem Int. 2013; 62: 731–737. doi: 10.1016/j.neuint.2012.10.013 PMID: 23142151

6. Bobermin LD, Quincozes-Santos A, Guerra MC, Leite MC, Souza DO, Gonçalves CA, et al. Resveratrol prevents ammonia toxicity in astroglial cells. PLoS One. 2012; 7: e52164. doi: 10.1371/journal.pone.0052164 PMID: 23284918

7. Shawcross DL, Wright G, Olde Damink SW, Jalan R. Role of ammonia and inflammation in minimal hepatic encephalopathy. Metab Brain Dis. 2007; 22: 125–138. PMID: 17260161

8. Nemeth E, Baird AW, O'Farrelly C. Microanatomy of the liver immune system. Semin Immunopathol. 2009; 31: 333–343. doi: 10.1007/s00281-009-0173-4 PMID: 19639317

9. Trauner M, Meier PJ, Boyer JL. Molecular pathogenesis of cholestasis. N Engl J Med. 1998; 339: 1217–1227. PMID: 9780343

10. Désert C, Duclos MJ, Blavy P, Lecerf F, Moreews F, Klopp C, et al. Transcriptome profiling of the feeding-to-fasting transition in chicken liver. BMC Genomics. 2008; 9: 611. doi: 10.1186/1471-2164-9-611 PMID: 19091074

11. Yang L, Tan GY, Fu YQ, Feng JH, Zhang MH. Effects of acute heat stress and subsequent stress removal on function of hepatic mitochondrial respiration, ROS production and lipid peroxidation in broiler chickens. Comp Biochem Physiol C Toxicol Pharmacol. 2010; 151: 204–208. doi: 10.1016/j.cbpc.2009.10.010 PMID: 19883793

12. Jia B, Yu ZJ, Duan ZF, Lü XQ, Li JJ, Liu XR, et al. Hyperammonaemia induces hepatic injury with alteration of gene expression profiles. Liver Int. 2014; 34: 748–758. doi: 10.1111/liv.12365 PMID: 24134218

13. Astle J, Ferguson JT, German JB, Harrigan GG, Kelleher NL, Kodadek T, et al. Characterization of proteomic and metabolomic responses to dietary factors and supplements. J Nutr. 2007; 137: 2787–2793. PMID: 18029500

14. Zhang JZ, Li DF. Effect of conjugated linoleic acid on inhibition of prolyl hydroxylase 1 in hearts of mice. Lipids Health Dis. 2012; 11: 22. doi: 10.1186/1476-511X-11-22 PMID: 22313584

15. Wang JJ, Li DF, Dangott LJ, Wu GY. Proteomics and its role in nutrition research. J Nutr. 2006; 136: 1759–1762. PMID: 16772433

16. Gebhardt R. Metabolic zonation of the liver: regulation and implications for liver function. Pharmacol Ther. 1992; 53: 275–354. PMID: 1409850

17. Kleinman MT, Araujo JA, Nel A, Sioutas C, Campbell A, Cong PQ, et al. Inhaled ultrafine particulate matter affects CNS inflammatory processes and may act via MAP kinase signaling pathways. Toxicol Lett. 2008; 178: 127–130. doi: 10.1016/j.toxlet.2008.03.001 PMID: 18420360

18. Huang J, Zhang Y, Zhou Y, Zhang Z, Xie Z, Zhang J, et al. Green tea polyphenols alleviate obesity in broiler chickens through the regulation of lipid-metabolism-related genes and transcription factor expression. J Agric Food Chem. 2013; 61: 8565–8572. doi: 10.1021/jf402004x PMID: 23992224

19. Diz AP, Truebano M, Skibinski DO. The consequences of sample pooling in proteomics: an empirical study. Electrophoresis. 2009; 30: 2967–2975. doi: 10.1002/elps.200900210 PMID: 19676090

20. Su L, Cao L, Zhou R, Jiang Z, Xiao K, Kong W, et al. Identification of novel biomarkers for sepsis prognosis via urinary proteomic analysis using iTRAQ labeling and 2D-LC-MS/MS. PLOS ONE. 2013; 8: e54237. doi: 10.1371/journal.pone.0054237 PMID: 23372690

21. Luo J, Zheng A, Meng K, Chang W, Bai Y, Li K, et al. Proteome changes in the intestinal mucosa of broiler (Gallus gallus) activated by probiotic Enterococcus faecium. J Proteomics. 2013; 91: 226–241. doi: 10.1016/j.jprot.2013.07.017 PMID: 23899589

22. Ramadoss J, Magness RR. Alcohol-induced alterations in maternal uterine endothelial proteome: a quantitative iTRAQ mass spectrometric approach. Reprod Toxicol. 2012; 34: 538–544. doi: 10.1016/j.reprotox.2012.08.008 PMID: 22960358

23. Shao C, Liu Y, Ruan H, Li Y, Wang H, Kohl F, et al. Shotgun proteomics analysis of hibernating arctic ground squirrels. Mol Cell Proteomics. 2010; 9: 313–326. doi: 10.1074/mcp.M900260-MCP200 PMID: 19955082

24. Olsen JV, Blagoev B, Gnad F, Macek B, Kumar C, Mortensen P, et al. Global, in vivo, and site-specific phosphorylation dynamics in signaling networks. Cell. 2006; 127: 635–648. PMID: 17081983

25. Hakimov HA, Walters S, Wright TC, Meidinger RG, Verschoor CP, Gadish M, et al. Application of iTRAQ to catalogue the skeletal muscle proteome in pigs and assessment of effects of gender and diet dephytinization. Proteomics. 2009; 9: 4000–4016. doi: 10.1002/pmic.200900049 PMID: 19701905

26. Ye J, Fang L, Zheng H, Zhang Y, Chen J, Zhang Z, et al. WEGO: a web tool for plotting GO annotations. Nucleic Acids Res. 2006; 34: W293–297. PMID: 16845012

27. Zi J, Zhang J, Wang Q, Zhou B, Zhong J, Zhang C, et al. Stress responsive proteins are actively regulated during rice (Oryza sativa) embryogenesis as indicated by quantitative proteomics analysis. PLOS ONE. 2013; 8: e74229. doi: 10.1371/journal.pone.0074229 PMID: 24058531

28. Nishikawa T, Bellance N, Damm A, Bing H, Zhu Z, Handa K, et al. A switch in the source of ATP production and a loss in capacity to perform glycolysis are hallmarks of hepatocyte failure in advance liver disease. J Hepatol. 2014; 60: 1203–1211. doi: 10.1016/j.jhep.2014.02.014 PMID: 24583248

29. Nikam A, Patankar JV, Lackner C, Schöck E, Kratky D, Zatloukal K, et al. Transition between acute and chronic hepatotoxicity in mice is associated with impaired energy metabolism and induction of mitochondrial heme oxygenase-1. PLOS ONE. 2013; 8: e66094. doi: 10.1371/journal.pone.0066094 PMID: 23762471

30. Young TA, Bailey SM, Van Horn CG, Cunningham CC. Chronic ethanol consumption decreases mitochondrial and glycolytic production of ATP in liver. Alcohol Alcohol. 2006; 41: 254–260. PMID: 16571619

31. Modrego J, de las Heras N, Zamorano-León JJ, Mateos-Cáceres PJ, Martín-Fernández B, Valero-Muñoz M, et al. Changes in cardiac energy metabolic pathways in overweighed rats fed a high-fat diet. Eur J Nutr. 2013; 52: 847–856. doi: 10.1007/s00394-012-0392-7 PMID: 22695689

32. Flowers MT. The delta9 fatty acid desaturation index as a predictor of metabolic disease. Clin Chem. 2009; 55: 2071–2073. doi: 10.1373/clinchem.2009.135152 PMID: 19850628

33. Nakamura MT, Nara TY. Structure, function, and dietary regulation of delta6, delta5, and delta9 desaturases. Annu Rev Nutr. 2004; 24: 345–376. PMID: 15189125

34. Yamada J. Long-chain acyl-CoA hydrolase in the brain. Amino Acids. 2005; 28: 273–278. PMID: 15731883

35. Witkowska D, Sowinska J, Iwanczuk-Czernik K, Mituniewicz T, Wojcik A, Szarek J. The effect of a disinfectant on the ammonia concentration on the surface of litter, air and the pathomorphological picture of kidneys and livers in broiler chickens. Arch Tierz Dummerstorf. 2006; 49: 249–256.

36. Pogorelova TN, Orlov VI, Gunko VO. New approaches to molecular diagnostics of prenatal pathology. Bull Exp Biol Med. 2011; 151: 567–570. PMID: 22462047

37. D'Aniello A, D'Onofrio G, Pischetola M, D'Aniello G, Vetere A, Petrucelli L, et al. Biological role of D-amino acid oxidase and D-aspartate oxidase. Effects of D-amino acids. J Biol Chem. 1993; 268: 26941–26949. PMID: 7903300

38. Ke Q, Yang RN, Ye F, Wang YJ, Wu Q, Li L, et al. Impairment of liver regeneration by the histone deacetylase inhibitor valproic acid in mice. J Zhejiang Univ Sci B. 2012; 13: 695–706. PMID: 22949360

39. Jagannathan M, Sakwe AM, Nguyen T, Frappier L. The MCM-associated protein MCM-BP is important for human nuclear morphology. J Cell Sci. 2012; 125: 133–143. doi: 10.1242/jcs.089938 PMID: 22250201

40. Yang X, Miao X, Wen Y, Hu J, Dai W, Yin B. A possible connection between adhesion regulating molecule 1 overexpression and nuclear factor kappa B activity in hepatocarcinogenesis. Oncol Rep. 2012; 28: 283–290. doi: 10.3892/or.2012.1767 PMID: 22576803

41. Maier KG, Han X, Sadowitz B, Gentile KL, Middleton FA, Gahtan V. Thrombospondin-1: a proatherosclerotic protein augmented by hyperglycemia. J Vasc Surg. 2010; 51: 1238–1247. doi: 10.1016/j.jvs.2009.11.073 PMID: 20299182

42. Newman DR, Kuhn JF, Shanab GM, Maxwell ES. Box C/D snoRNA-associated proteins: two pairs of evolutionarily ancient proteins and possible links to replication and transcription. RNA. 2000; 6: 861–879. PMID: 10864044

43. Chaika NV, Yu F, Purohit V, Mehla K, Lazenby AJ, DiMaio D, et al. Differential expression of metabolic genes in tumor and stromal components of primary and metastatic loci in pancreatic adenocarcinoma. PLOS ONE. 2012; 7: e32996. doi: 10.1371/journal.pone.0032996 PMID: 22412968

44. Bertrand FE, Billips LG, Gartland GL, Kubagawa H, Schroeder HW Jr. The J chain gene is transcribed during B and T lymphopoiesis in humans. J Immunol. 1996; 156: 4240–4244. PMID: 8666793

45. Varki A, Cummings RD, Esko JD, Freeze HH, Stanley P, Bertozzi CR, et al. Essentials of Glycobiology. 2nd edition. Cold Spring Harbor, NY: Cold Spring Harbor Laboratory Press; 2009.

46. Reinitz E, Lawrence M, Diamond B, Keiser H, Alper C. Arthritis and antinuclear antibodies (ANA) with inherited deficiency of the sixth component of complement (C6). Ann Rheum Dis. 1986; 45: 431–434. PMID: 3487293

47. Saller E, Tom E, Brunori M, Otter M, Estreicher A, Mack DH, et al. Increased apoptosis induction by 121F mutant p53. EMBO J. 1999; 18: 4424–4437. PMID: 10449408

48. Choi HY, Chong SA, Nam MJ. Resveratrol induces apoptosis in human SK-HEP-1 hepatic cancer cells. Cancer Genomics Proteomics. 2009; 6: 263–268. PMID: 19996131

49. Esbaugh AJ, Tufts BL. The structure and function of carbonic anhydrase isozymes in the respiratory system of vertebrates. Respir Physiol Neurobiol. 2006; 154: 185–198. PMID: 16679072

50. Polyzos SA, Kountouras J, Zavos C, Papatheodorou A, Katsiki E, Patsiaoura K, et al. Serum ferritin in patients with nonalcoholic fatty liver disease: evaluation of ferritin to adiponectin ratio and ferritin by homeostatic model of assessment insulin resistance product as non-invasive markers. Immuno-Gastroenterology. 2012; 1: 119–125.

51. Yoo DR, Chong SA, Nam MJ. Proteome profiling of arsenic trioxide-treated human hepatic cancer cells. Cancer Genomics Proteomics. 2009; 6: 269–274. PMID: 19996132

52. Scheri RC, Lee J, Barofsky DF, Curtis LR. Chlordecone increased subcellular distribution of scavenger receptor class B type II to murine hepatic microsomes without altering cytosolic cholesterol binding proteins. Toxicol Lett. 2009; 191: 20–25. doi: 10.1016/j.toxlet.2009.07.029 PMID: 19666090

53. Serra MP, Marongiu F, Sini M, Marongiu M, Contini A, Wolff H, et al. Hepatocyte senescence induced by radiation and partial hepatectomy in rat liver. Int J Radiat Biol. 2014; 90: 876–883. doi: 10.3109/09553002.2014.922714 PMID: 24827852

54. St Peter SD, Imber CJ, De Cenarruzabeitia IL, McGuire J, James T, Taylor R, et al. Beta-galactosidase as a marker of ischemic injury and a mechanism for viability assessment in porcine liver transplantation. Liver Transpl. 2002; 8: 21–26. PMID: 11799481

55. Chen JY, Chou HC, Chen YH, Chan HL. High glucose-induced proteome alterations in hepatocytes and its possible relevance to diabetic liver disease. J Nutr Biochem. 2013; 24: 1889–1910. doi: 10.1016/j.jnutbio.2013.05.006 PMID: 24011924

56. Matsumoto T, Kinoshita T, Matsuzaka H, Nakai R, Kirii Y, Yokota K, et al. Crystal structure of non-phosphorylated MAP2K6 in a putative auto-inhibition state. J Biochem. 2012; 151: 541–549. doi: 10.1093/jb/mvs023 PMID: 22383536

57. Nakagawa H, Maeda S. Molecular mechanisms of liver injury and hepatocarcinogenesis: focusing on the role of stress-activated MAPK. Patholog Res Int.; 2012. Article ID: 172894. 14 p.

58. Wagner EF, Nebreda AR. Signal integration by JNK and p38 MAPK pathways in cancer development. Nat Rev Cancer. 2009; 9: 537–549. doi: 10.1038/nrc2694 PMID: 19629069

59. Dixit SS, Jadot M, Sohar I, Sleat DE, Stock AM, Lobel P. Loss of Niemann-Pick C1 or C2 protein results in similar biochemical changes suggesting that these proteins function in a common lysosomal pathway. PLOS ONE. 2011; 6: e23677. doi: 10.1371/journal.pone.0023677 PMID: 21887293